LBL-3434
c.2

Presented at Symposium on Classical and
Quantum Mechanical Aspects of Heavy
Ion Collisions, Heidelberg, Germany,
October 2-4, 1974

THE ANALYSIS OF HIGH ENERGY HEAVY-ION TRANSFER REACTIONS

D. K. Scott

November, 1974

Prepared for the U. S. Atomic Energy Commission
under Contract W-7405-ENG-48

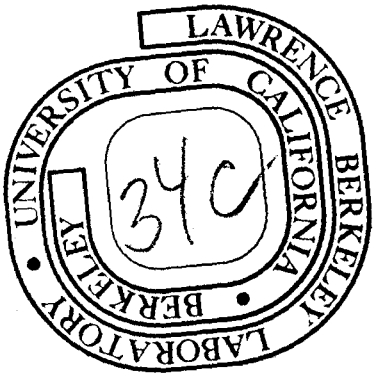

LBL-3434
c.2

DISCLAIMER

THE ANALYSIS OF HIGH ENERGY HEAVY-ION TRANSFER REACTIONS*

D. K. Scott
Lawrence Berkeley Laboratory
University of California
Berkeley, California 94720

ABSTRACT

The regions of validity of quantal and semiclassical theories are discussed for high energy transfer reactions with heavy-ions. After demonstrating the equivalence of the two formalisms, they are applied quantitatively to predict spectroscopic factors, the energy dependence and Q dependence of single nucleon transfer on lead. The power of semiclassical theory for making wide surveys is shown. The discovery of simple cluster states in multinucleon transfer reactions on lighter nuclei is discussed using semiclassical theory. Finally the quantal analysis of new effects due to multistep processes in high energy heavy-ion reactions is presented.

1. Introduction

The rapid advances in experimental heavy-ion physics have sparked off a remarkable inventiveness among theoreticians in developing new reaction theories and interpretations of the data. These range from simple qualitative semiclassical insights to formal semiquantal theories, and to a bewildering variety of approximations to make the exact quantum mechanical theories amenable to calculations. In two years the field has evolved from the viewpoint that heavy-ion reactions were beautifully simple, to one implying that the proper interpretation is of staggering complexity. This conference may show us that the simplicities are still there after all. We should not be too elated at the successes of the simple theories, nor despair at the failures of the complicated theories. The lesson to be learned from the last few years and from this conference was learned long ago on the English Public School playing fields: "It matters not who won or lost, but how they played the game." This talk is about some of the games that have been played in interpreting high energy heavy-ion transfer data from quantum mechanical and semiclassical approaches. Some general aspects of these approaches and the effect on differential cross sections are discussed in the next section. In section 3, both methods are applied to single nucleon transfer data on ^{208}Pb, which serves as a standard of calibration and of comparison for different theories. This is followed in section 4 by a discussion of transfers on lighter nuclei, where the semiclassical approach is on less sure ground, but where we show that it can give physical insight, and suggest interesting experiments. In section 5 we discuss multistep processes at high energy, for which so far only the

quantum mechanical calculations have been done; the results are sufficently exciting to make us hope that the development of a semiclassical theory will be forthcoming in order to make surveys of the type discussed in sections 3 and 4. Our conclusions are presented in section 6.

2. General Semiclassical and Quantum Mechanical Aspects of High Energy Data

A characteristic feature of high energy heavy-ion reactions is that the wave length of relative motion ($\lambda\!\!\!^{-}$) is very short compared to the nuclear radii. Typically for ^{16}O ions of 10 MeV/nucleon on ^{208}Pb, $\lambda\!\!\!^{-} \approx 0.2$ fm compared to $R_1 + R_2 \approx 13$ fm. This localisation leads to the concept of a well-defined classical trajectory. It is important to remember, however, that the classical picture arises from the interference of a large number of waves[1], and therefore the concept of a trajectory is valid only under the condition that the beam contains a sufficiently large number of orbital angular momenta ($\Delta\ell$), which however must still be small compared to the grazing orbital angular momentum (ℓo). Only then exists the possibility of defining phase shifts and Legendre Polynomials as smooth functions of ℓ, and the replacement of quantized sums by integrals. An example is shown[2] in fig. 1, for the reaction of 100 MeV ^{18}O ions on Sn, where S_ℓ the amplitude in the outgoing channel is plotted as a function of ℓ. In this case the semiclassical condition might be satisfied, with $\ell o \approx 57\ \hbar$ and $\Delta\ell \approx 15\hbar$ (evaluated at 1/e of the maximum).

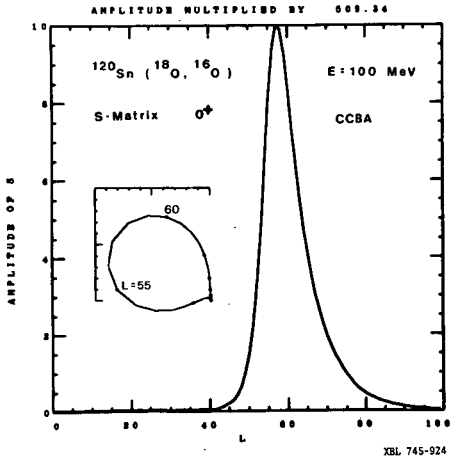

Fig. 1. The amplitude of the S-matrix for the ground state transition in the reaction $^{120}Sn(^{18}O,^{16}O)^{122}Sn$ at 100 MeV. The inset shows S plotted in the complex plane, its real part on the x-axis. The positions of ℓ = 55 and 60 are marked.

The orbit concept also requires that the uncertainty in the angle of scattering $\Delta\Theta$, should be small compared to Θ. Now we can write $\Theta \approx \frac{\Delta p}{p}$, where p is the incident momentum and the change is Δp. So $\Theta \approx \int \frac{F dt}{p}$, where F, the force acting on the particle over the region "a", is V/a, and $dt \approx a/v$, so $\Theta \approx V/E$. When the particle passes through the region "a" the uncertainty in the transverse momentum is $\delta p \approx \hbar/a$, and so $\Delta\Theta \approx \hbar/ap$; and finally $\Theta/\Delta\Theta \approx \frac{Va}{\hbar v}$, which we require to be much greater than unity. This condition is better satisfied the lower the energy. On the other hand the condition $\lambda\!\!\!^{-} \ll R_1 + R_2$ is fulfilled better at high incident energy. It is important therefore to have a more general criterion for the degree of "classicality" of a reaction.

We write the scattering amplitude,

$$f(\Theta) = \frac{1}{2ik} \sum (2\ell+1)\ \eta_\ell\ e^{2i\delta_\ell}\ P_\ell(\cos\Theta) \tag{1}$$

and the reaction amplitude, assuming the peripheral nature of the reaction, as a Gaussian distribution[3] (justified by the output of "exact" DWBA calculations e.g. see fig. 1)

$$\eta_\ell = \eta_{\ell o}\ \ \text{EXP}\ \ -\left[\frac{(\ell-\ell_o)^2}{(\Delta\ell)^2}\right] \tag{2}$$

$P_\ell(\cos\Theta)$ is replaced by the asymptotic expression valid for large ℓ, and $\sin\Theta > 1/\ell$,

$$P_\ell(\cos\Theta) \approx [1/2(\ell+1/2)\ \pi\ \sin\Theta]^{-1/2}\ \ \sin[(\ell+1/2)\Theta + \pi/4] \tag{3}$$

For δ_ℓ we make the Taylor expansion:

$$\delta_\ell = \delta_{\ell o} \pm \left(\frac{d\delta}{d\ell}\right)_{\ell=\ell o}(\ell-\ell o) + 1/2\left(\frac{d^2\delta}{d\ell^2}\right)_{\ell=\ell o}(\ell-\ell o)^2 + \ldots\ldots\ldots \tag{4}$$

On account of the WKB classical relationship[4] for the scattering angle Θ_ℓ corresponding to partial wave ℓ,

$$\Theta_\ell = 2\,\frac{d\delta_\ell}{d\ell} \tag{5}$$

we can write

$$\delta_\ell = \delta_{\ell o} \pm \frac{\Theta_o}{2}\ (\ell-\ell o) + 1/4\left(\frac{d\Theta\ell}{d\ell}\right)_{\ell=\ell o}(\ell-\ell o)^2 + \ldots\ldots\ldots \tag{6}$$

where Θ_o is the classical angle of deviation for the tangetial trajectory (not necessarly purely Coulomb). Substituting in (1) and converting the summation to an integral gives

$$\frac{d\sigma}{d\Omega} = |f(\Theta)|^2 \ \alpha\ \text{EXP}\ \left\{\frac{-(\Theta-\Theta_o)^2}{(\Delta\Theta)^2}\right\} + \text{EXP}\ \left\{\frac{-(\Theta+\Theta_o)^2}{(\Delta\Theta)^2}\right\} + \left(\begin{matrix}\text{INTERFERENCE}\\ \text{TERM}\end{matrix}\right) \tag{7}$$

For the sake of historical accuracy it is worth noting that the interference term was present in the early treatments of high energy heavy-ion transfer[3,5,6] theories but it was always averaged over, because the data were too crude at that time. Kahana et al.[7] interpret the differential cross section as the interference of two classical distributions centered at the physical angle (Θ_o) and the unphysical ($-\Theta_o$). Here we discuss only the term

$$\frac{d\sigma}{d\Omega}\ \alpha\ \text{EXP}\left[\frac{-(\Theta-\Theta_o)^2}{(\Delta\Theta)^2}\right], \tag{8}$$

since so far no high energy data has revealed the interference oscillations. They remain a challenge to experimental ingenuity. This equation describes a symmetric distribution of width[8]:

$$(\Delta\theta)^2 = \frac{2}{(\Delta\ell)^2} + \frac{1}{2}\left(\frac{d\theta_\ell}{d\ell}\right)^2 (\Delta\ell)^2 \qquad (9)$$

Thus for small $\Delta\ell$ the distribution is broad due to quantal dispersion, and if $\Delta\ell$ is very large the distribution is also broad due to "dynamic" dispersion. The minimum value of $(\Delta\theta)$ is obtained for

$$\Delta\ell = \sqrt{2\left(\frac{d\ell}{d\theta}\right)_{\ell_o}} = \sqrt{\eta} \quad \mathrm{cosec}\left(\frac{\theta_o}{2}\right), \qquad (10)$$

where η is the sommerfeld parameter. Using the classical result $\ell=\eta \cot\left(\frac{\theta}{2}\right)$ (11)

then

$$(\Delta\theta)_{MIN} = \frac{2}{\sqrt{\eta}} \sin\left(\frac{\theta_o}{2}\right). \qquad (12)$$

If $(\Delta\ell)^2 \gg \mathrm{cosec}^2\left(\frac{\theta_o}{2}\right)$ we have a classical situation, and the width of $\Delta\theta$ increases with $\Delta\ell$, but if $(\Delta\ell)^2 \ll \eta\ \mathrm{cosec}^2\left(\frac{\theta_o}{2}\right)$, we have a quantum situation and as $\Delta\ell$ increases, $\Delta\theta$ decreases[9].

If we take as an example the data of fig. 1, $\Delta\ell$ is derived independently from a quantum mechanical calculation using a correct form factor and optical parameters pertinent to elastic scattering[2]. The value of 225 for $(\Delta\ell)^2$ is approximately the same as $\eta\ \mathrm{cosec}^2(\theta/2) \approx 200$. These data correspond therefore to the region of the minimum $\Delta\theta$, and are in the transitional region between classical and quantum descriptions. A consideration of the data from both viewpoints is likely to be instructive. Further if we consider the single nucleon transfer data[10,11] on Pb shown in fig. 2, at 98 MeV, the classical conditions are better satisfied. On the figure we show the value of $(\Delta\theta)_{MIN}$ and the value of θ_o predicted from the equation

$$\mathrm{cosec}\left(\frac{\theta_o}{2}\right) = \frac{2E\ (R_1+R_2)}{z_1 z_2 e^2} - 1 \qquad (13)$$

It is interesting that this formula predicts that the grazing angle, taken as an average over the initial and final orbits, should move to large angles with increasing excitation energy (as E in the final channel decreases). This effect is observed in fig. 2(a) for neutron transfer, and is predicted by DWBA for the proton transfer in fig. 2(b), although in this case the position of the experimental peak is in fact constant. This disagreement, which is greatest for the case of lowest angular momentum transfer has been discussed by von Oertzen[12]. If we write the initial and final angular momenta

$$\ell_i = \eta_i \cot\left(\frac{\theta_o^i}{2}\right), \quad \ell_f = \eta_f \cot\left(\frac{\theta_o^f}{2}\right) \qquad (14)$$

then the requirement that $\ell_i \approx \ell_f$, together with the fact that $\eta_f < \eta_1$ in proton

stripping, implies $\theta_f < \theta_i$, and that the absorption and hence the position of the classical maximum are determined primarily by the initial orbit. This effect has been reproduced by (somewhat artificial) adjustment of optical parameters[13,14]. Probably there are subtleties of the heavy-ion potential as yet unaccounted for.

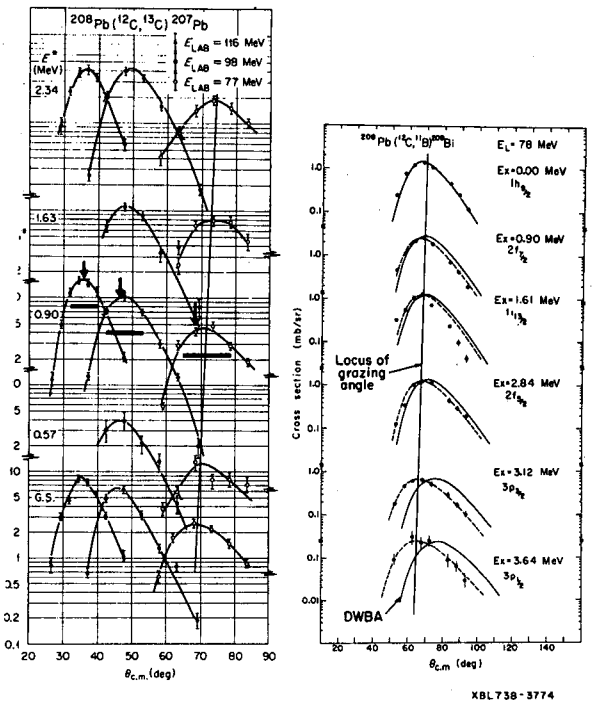

Fig. 2. (a) differential cross sections for the $^{208}Pb(^{12}C,^{13}C)^{207}Pb$ reaction leading to single hole states at incident energies of 77, 98, and 116 MeV. The bold arrows denote the grazing angle predicted by eq. 13. The locus of this angle as a function of energy is indicated. The bold horizontal lines are the minimum FWHM of the distributions, predicted from eq. 12. (b) differential cross sections for the $^{208}Pb(^{12}C,^{11}B)^{209}Be$ reaction at 78 MeV. The dotted lines are drawn through the data points, and the solid curves are DWBA predictions.

The characteristic feature of the distribution function derived by expanding δ_ℓ to second order in $(\ell-\ell_o)$ is that it is symmetrical about θ_o. The data in fig. 3 for one and two nucleon transfer on Nd, from Berkeley illustrate another effect. The one nucleon transfer data has a symmetric peak of width somewhat larger than the estimate of eq. 12, and in fact this reaction meets the semi-classical criteria. On the other hand the peak for two nucleon transfer is considerably broadened and asymmetric. Shown in the figure are two DWBA analyses using the optical model parameters[15,16] of Table 1. For one nucleon transfer the predictions are almost identical, whereas there is a factor of ten between the predictions at forward angles for two nucleon transfer. Glendenning and Ascuitto[17] have discussed how the sharper fall-off of the two nucleon form factor, makes the forward cross section particularly sensitive to close trajectories, and consequently they provide a probe of the nuclear edge, and of the relationship between the imaginary and the real potentials.

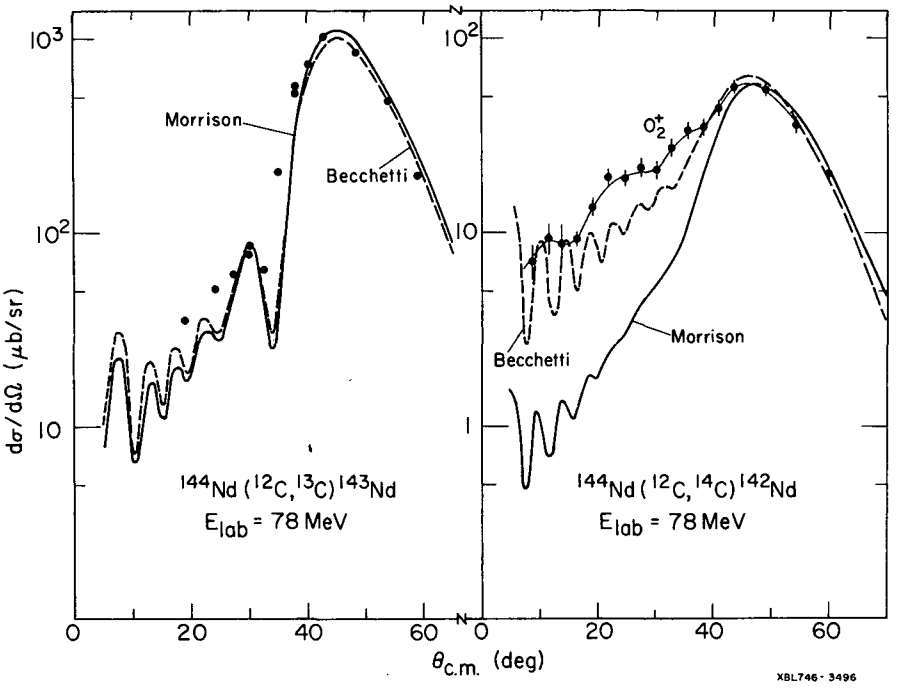

Fig. 3. Differential cross sections for the reactions ^{144}Nd(^{12}C,^{13}C)^{143}Nd and ^{144}Nd(^{12}C,^{14}C)^{142}Nd at 78 MeV. Two sets of DWBA calculations are shown using the optical model parameters of Table 1. These give almost identical results for one nucleon transfer, but are makedly different for two nucleon transfer. (The calculation for (^{12}C,^{14}C) with the Morrison potential used different real and imaginary diffuseness of 0.49 and 0.6 fm. In the (^{12}C,^{13}C) these parameters would lower the forward cross section by approximately a factor of 2, but does not effect our conclusions in the text).

Table 1. Optical model parameters used in the analysis of one and two nucleon transfer reactions on ^{144}Nd.

	V	W	r_o	a	r_c
Morrison (ref. 16)	-100	-40	1.22	0.5	1.2
Becchetti (ref 15)	- 40	-15	1.31	0.45	1.2

How do we interpret such an asymmetry semiclassically? Recently it has been shown[18] that if we expand δ_ℓ to third order,

$$\delta_\ell = \delta_{\ell o} + \left(\frac{\Theta_o}{2}\right)(\ell-\ell_o) + \ldots + \frac{1}{3}\beta\,(\ell-\ell_o)^3 \qquad (15)$$

the resultant $|f(\Theta)|^2$, takes on the form shown by $|g(\Theta)|^2$ in fig. 4, where the cross section for the physical scattering becomes tipped to more forward angles, and takes on the form of the Airy function. The effect on the deflection function of a third order term in δ_ℓ is

$$\Theta_\ell = 2\frac{d\delta_\ell}{d\ell} = \Theta_o + \ldots + \beta(\ell-\ell_o)^2 \qquad (16)$$

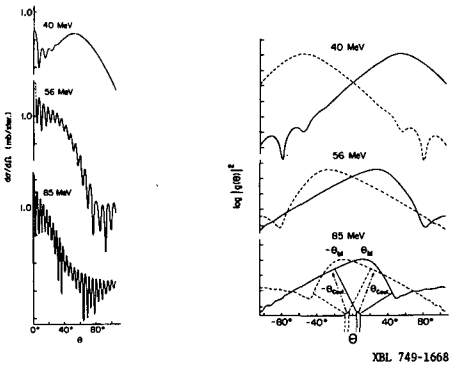

Fig. 4. On the right are shown single-slit diffraction-refraction patterns from DWBA calculations for the reaction $^{48}Ca(^{16}O,^{14}C)^{50}Ti$ (shown on the left). The two distributions correspond to the grazing angle distributions centered at the physical angle Θ_M and the unphysical $-\Theta_M$. (compare eq. 7). At 85 MeV the distributions take on an asymmetric form. (see the discussion of of eq. 15).

i.e. it adds a parabolic dip, deviating the deflection angle for trajectories passing through the ℓ-window. The physics of this "refraction" is obviously closely related to the optical potential. The interesting insights will come from such associations of the parameters of the semi-classical expansion with the optical model of the heavy-ion interaction. Fig. 4 shows how at high energy the overlap of the two asymmetric distributions leads to a modulation of the diffractive oscillations. It is also interesting to note the existence of gross oscillations in fig. 3 for two nucleon transfers, which, in the light of past experiences, we should perhaps not ignore.

Finally it is amusing to note that kinks, and modulations in deflection functions and phase shifts are not entirely new in the subject of heavy-ion physics. Fig. 5 illustrates an early calculation[5] for the multinucleon transfer reaction (Ne^{20}, Na^{24}) on Au, where the discontinuty between the initial and final orbits leads to an unusual average deflection function in the region where the reaction amplitude for multinucleon transfer is concentrated. The phase shift as a function of ℓ develops inflexions and the differential cross section becomes double peaked.

3. DWBA and Semiclassical Theories Applied to High Energy Transfer Data on Pb

Before discussing the formal DWBA and semiclassical theories applied to high energy transfer data, it is worthwhile recalling the main features of the data which stimulated their development. The work of the Berkeley group for (^{16}O,^{15}N) on ^{208}Pb from 104 to 216 MeV is shown[19] in fig. 6. The variety of pure single particle states excited makes this reaction a standard of comparison and calibration of different reaction theories. The striking feature is the dominance of the $j_f = l_f + 1/2$ state at low energy and the equality of $l_f \pm 1/2$ at the highest energy, the understanding of which brought about a revolution in reaction theories for heavy-ions. From an intuitive viewpoint the effect is easily understood as the overcoming of the orbital velocity by the velocity of the transferred particle due to the projectile motion (see fig. 6), whereas for low projectile velocity a smooth transition selects a final $j_f = l_f + 1/2$ from an initial $j_i = l_i - 1/2$.

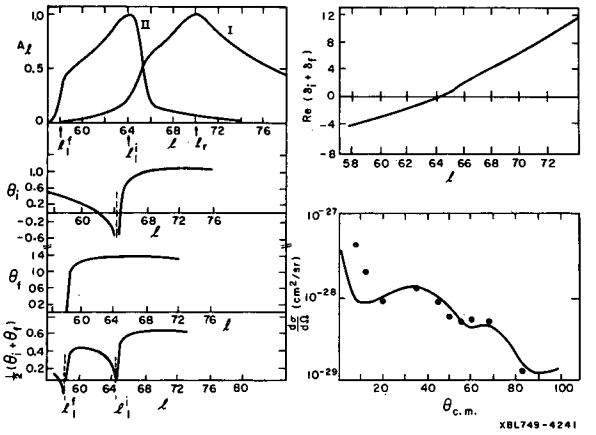

Fig. 5. The top figure shows the amplitude for single nucleon (I) and multinucleon (II) transfer induced by ^{20}Ne on ^{197}Au at E_{CM} = 127 MeV. The multinucleon transfer (^{20}Ne,^{24}Na) is peaked at smaller ℓ-values. Underneath are the deflection functions for the initial and final channels, together with the average $1/2(\Theta_i+\Theta_f)$. The corresponding phase shift is plotted at the top right. The differential cross section below has a double maximum, due to the discontinuities between the initial and final channels of the multinucleon transfer.

The formalisms of DWBA and SC theory will now be described to show their relationship. Their quantitative agreement is compared by applying these theories to various features of the data, such as spectroscopic factors, energy dependence and Q-dependence.

3.1 DWBA Formalism

The relevant vector diagram for the reaction A(a,b)B with a = b + x and B = A + x is shown in fig. 7. For single nucleon transfer the transition probability involves the six-dimensional integration over $\underline{r}_i$, $\underline{r}_f$

$$T^{DWBA} = \int \underline{dr}_f \, \underline{dr}_i \, \chi_f^* \, (\underline{k}_f, \underline{r}_f) \, \phi_B^* \, (\underline{r}_2) \, V\phi_a(\underline{r}_i) \, \chi_i \, (\underline{k}_i, \underline{r}_i) \qquad (17)$$

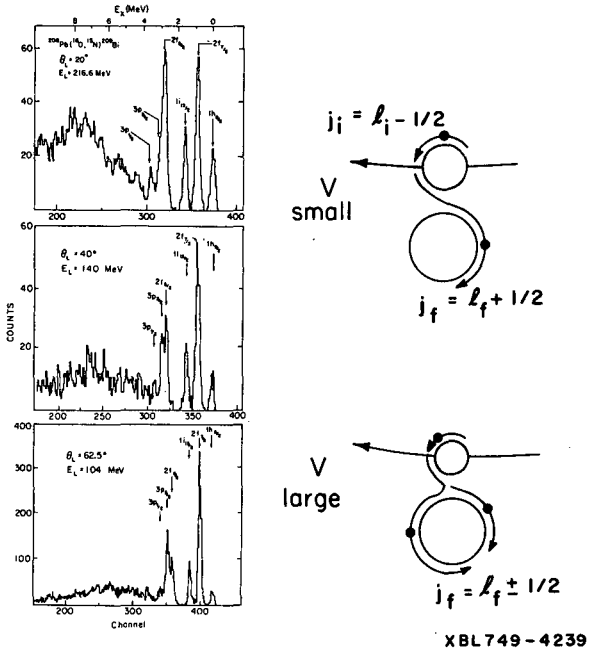

Fig. 6. Energy spectra for the reaction ^{208}Pb (^{16}O,^{15}N)^{209}Bi at 104, 140 and 216 MeV. At the lowest energy the reaction favors $j_f = \ell_f + 1/2$ over $j_f = \ell_f - 1/2$, whereas at the highest energy they are equal. The figure at the right explains the phenomenon in terms of orbit matching at low and high velocity.

The χ's are distorted waves, and the ϕ's represent wave functions of the relative motions of the nucleon x bound to the cores A or b. In general one must also include spectroscopic amplitudes Θ_i, Θ_f for the decomposition A → b + x, B → A + x. In the post representation $V = V_{bB} - U_{bB}$, the difference between the total interaction in the final channel and the average interaction of the optical potential, and is approximately $V_{bx}(\underline{r}_1)$; in the prior representation, it is $V_{Ax}(\underline{r}_2)$. A plethora of methods exist for approximating this integral (see the discussion in refs. 20, 21), the most drastic of which is the "no-recoil" approximation obtained by ignoring the difference between $\underline{r}_f$ and $\underline{r}_i$. In order to show the relationship to the semi-classical theory we derive this approximation by setting $\underline{r}_f \approx \frac{A}{B}\underline{r}$ and $\underline{r}_i \approx \underline{r}$. Then

$$T^{DWBA} = \int \chi_f^*(\underline{k}_f, \frac{A}{B}\underline{r})\ F(\underline{r})\ \chi_i(\underline{k}_i, \underline{r})\ d\underline{r} \tag{18}$$

$$F(r) = \int \phi_B^*(\underline{r} + \underline{r}')\ V_{bx}(\underline{r}')\ \phi_a(\underline{r}')\ d\underline{r}' \tag{19}$$

and we obtain two three-dimensional integrals. The effect of this approximation can be seen[22] by expanding the distorted waves,

$$\chi(\underline{k}, \underline{r} + \delta\underline{r}) = e^{\delta\underline{r}\cdot\nabla}\ \chi(\underline{k},\underline{r}) \tag{20}$$

$$\approx e^{\delta\underline{r}\cdot K(\underline{r})}\ \chi(\underline{k},\underline{r})$$

where $K(\underline{r})$ is the local momentum vector at point $\underline{r}$. Then eq. (17) reduces to the form of eq. 18 with F replaced by

$$F(\underline{r}) = \int e^{iP(\underline{r})\cdot\underline{r}'}\ \phi_B^*(\underline{r} + \underline{r}')\ V_{bx}(\underline{r}')\ \phi_a(\underline{r}')\ \underline{dr}' \tag{21}$$

and

$$P(\underline{r}) = \frac{x}{B} K_f(\underline{r}) + \frac{x}{a} K_i(\underline{r}) \tag{22}$$

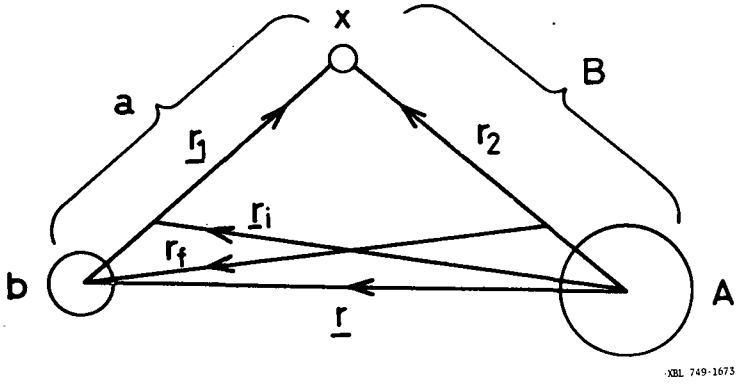

Fig. 7. Vector diagram for the reaction A(a,b)B with a = b + x and B = A + x. The relative coordinates of the colliding nuclei in the initial and final channels are $\underline{r}_i$, $\underline{r}_f$, and $\underline{r}$ is the relative seperation of the cores. The coordinate of the transferred particle x in the incident and residual nuclei is represented by $\underline{r}_1$, $\underline{r}_2$.

or in terms of velocities, since

$$\underline{k}_f = \frac{(A + x)b}{A + x + b}\ \frac{\underline{v}_f}{\hbar} \quad \text{and} \quad \underline{k}_i = \frac{(b + x)A}{A + x + b}\ \frac{\underline{v}_i}{\hbar} \tag{23}$$

$$p \approx \frac{x(A\underline{v}_i + b\underline{v}_f)}{\hbar(A + x + b)} \approx \frac{x\overline{v}}{\hbar}\ . \tag{24}$$

were $\overline{v}$ is an average of the initial and final velocities.

The classical picture shows the main contribution to the reaction came from distances of order sum of the nuclear radii, so therefore $\underline{r}' \approx R_a$, the projectile radius. The recoil term introduces additional angular momentum transfers of order $\underline{P}\cdot\underline{R}_a$ which is the angular momentum carried by the transferred particle due to the projectile motion at the surface. It also allows unnatural party terms through, for example, the first term in the expansion

$$e^{i\underline{P}\cdot\underline{r}'} = 1 + i\underline{P}\cdot\underline{r}' + \ldots\ldots\ldots \tag{25}$$

The corresponding selection rules[22] for a transition in the no-recoil approximation from a state $(l_1 j_1)$ to $(l_2 j_2)$ are:

$$|\ell_1 - \ell_2| \leq \Delta\ell \leq \ell_1 + \ell_2$$
$$|j_1 - j_2| \leq \Delta\ell \leq j_1 + j_2 \qquad (26)$$
$$(-1)^{\Delta\ell} = (-1)^{\ell_1 + \ell_2}$$

The last rule is relaxed when the additional transfers are permitted in the full recoil treatment. For example in a transition from p 1/2 → f 7/2, Δl = 3,4 and from p 1/2 → f 5/2, Δl = 2,3. In the no recoil approximation only 4 and 2 are permitted which has the effect of enhancing the f 7/2 state at the lower energy (see fig. 6) since high angular momentum transfers are favored.

Many techniques have been developed for the evaluation of the DWBA integral without making the no-recoil approximation. They have been reviewed recently by Glendenning and Nagarajan[21] and by Blair et al.[20] We shall defer a comparison of the results until we also develop the basic semiclassical transition amplitude.

3.2 Semiclassical Theory for High Energy Reactions

Under the conditions outlined in section 2, it was shown that for many reactions, there is a well-localized trajectory. Then the transition amplitude can be evaluated by integration of the quantum mechanical matrix element along the orbit.[23,24] Using the same notation as for the DWBA, the nucleon x starts out at $t = -\infty$ in a bound state of the potential V_1 provided by the moving core b. We must calculate the probability that the nucleon transfers to a bound state of the potential V_2 of the core A at $t = \infty$.

$$T^{SC} = \frac{1}{\hbar} \int \langle \psi_B \, V_{\psi a} \rangle \, dt. \qquad (27)$$

where the wave functions refer to bound states of the particle in moving potentials. In the transformation to a stationary frame:

$$\langle \psi_B \, V \psi_a \rangle = F(t) \, \mathrm{EXP} \left\{ \frac{-i}{\hbar} \left[Q + \frac{1}{2} x \dot{\underline{r}}^2 \right] \right\} \qquad (28)$$

$$F(t) = e^{\frac{i}{\hbar} x \dot{\underline{r}} \cdot \underline{r}'} \, \phi_B[\underline{r}(t) + \underline{r}'] \, V(\underline{r}') \, \phi_a(\underline{r}') \, d\underline{r}' \qquad (29)$$

Here Q is the reaction Q value modified by the change in Coulomb energy $(Z_1^f Z_2^f - Z_1^i Z_2^i) e^2/R$ in charge transfer; $\underline{r}(t)$ is the relative separation of the cores, and $\underline{r}'$ is the coordinate of x relative to core b.

Obviously F(t) in eq. (29) is closely related to F(r) in eq. (21) in view of eq. (24), while the phase factor $(Q + 1/2) \times \dot{\underline{r}}^2$ replaces the distorted wave integral

in eq. (18). This becomes clear when the reaction Q-value is expanded to first order in $(\underline{k}_f - \underline{k}_i)$ and the mass of the transferred particle x.

$$Q = \delta\left(\frac{\hbar^2 k^2}{2\mu}\right) \approx \hbar v_i (k_f - k_i) - \frac{1}{2}\hbar\,(v_i k_i)\,\frac{\delta\mu}{\mu} \tag{30}$$

where μ is the reduced mass. Setting $\frac{\delta\mu}{\mu} \approx \frac{x(b - A)}{b + A}$ leads to

$$Q \approx \hbar v_i (k_f - k_i + \frac{x}{b} k_i) - \frac{1}{2} x v_i^2 \tag{31}$$

$$\therefore \hbar v_i (k_f - k_i) \approx Q + \frac{1}{2} x v_i^2 \tag{32}$$

and $$r.(k_f - k_i) \approx \frac{t}{\hbar}(Q + \frac{1}{2} x v_i^2).$$

which relates the phase factor of the distorted waves to that of the semiclassical expression. The two evaluations of the transition probability essentially contain the same physics as required by the correspondence principle. We shall now see how well they compare in describing the experimental data.

3.3 Comparison of SC and DWBA for High Energy Single Nucleon Transfer on Pb

In principle the DWBA and semiclassical integrals can be evaluated exactly, but to economize on computing time a number of approximations have been developed.[20,21] For the DWBA Nagarajan has used a first order expansion[25] of the recoil phase factor in eq. (25), a method extended by Kahana and Baltz to higher orders[26]. More accurate methods are discussed by Elbaz et al.[27] The expansion to first order can seldom be justified at high energies as the expansion parameter usually exceeds unity. The semiclassical formulation has the advantage that the recoil term can be included exactly if the bound state wave function is approximated by a Hankel function[24]. Other novel techniques have been the direct evaluation of the multidimensional integral using Montecarlo techniques[28], or expansion of the distorted waves in a plane wave series to achieve separation of coordinates[29]. Low and Tamura point out the saving in computer time of using interpolation to evaluate the slowly varying form factor from points calculated on a coarser mesh than the rapidly varying distorted waves[13,30].

Some comparisons of these methods for the reaction $^{208}Pb(^{16}O,^{15}N)^{209}Bi$ are shown in Tables 2 and 3. The semiclassical calculations were made by integrating along a hyperbolic orbit, corresponding to a grazing collision, since differential cross sections have not been treated so far. (This would require taking into account the effect on the trajectory of the nuclear and absorptive potentials[31]). The tables show that the methods of including recoil give an agreement within a factor of approximately two for the spectroscopic factors. The Oak Ridge group have also made a study of ^{11}B induced reactions on Pb using the "exact" approach and conclude[14] that effects due to optical potentials, normalisations, finite-range and non-locality may

Table II. Spectroscopic factors for the reaction $^{208}Pb(^{16}O,^{15}N)^{209}Bi$ at 104 MeV.

Method \ State	$h_{9/2}$	$f^{*}_{7/2}$	$i_{13/2}$	$f_{5/2}$	$p_{3/2}$	$p_{1/2}$
No-recoil[a]	4.80	1.00	0.83	4.00	1.15	3.50
Nagarajan[a]	1.32	1.00	0.80	1.12	1.28	0.82
Tamura[b]	1.29	1.00	-	0.92	0.79	0.61
Semiclassical[c]	0.71	1.00	1.12	1.10	1.26	0.78
Exact[d]	2.60	1.00	0.96	1.48	1.48	0.60-1.00

*Spectroscopic factors are normalized to unity for the f 7/2 state.

[a]D. G. Kovar et al. Phys. Rev. Lett. 30 (1973) 1075

[b]Ref. 30;

[c]Refs. 24 and 33

[d]Ref. 19.

Table III. Spectroscopic factors for the reaction $^{208}Pb(^{16}O,^{15}N)^{209}Bi$ at 140 MeV.

Method \ State	$h_{9/2}$	$f^{*}_{7/2}$	$1_{13/2}$	$f_{5/2}$	$p_{3/2}$	$p_{1/2}$
No-recoil[a]	8.00	1.00	0.83	6.67	1.00	6.20-10.0
Nagarajan[a]	2.77	1.00	0.84	1.35	1.04	1.47
Tamura[b]	1.42	1.00	-	0.81	0.79	0.83
Semiclassical[c]	0.96	1.00	0.74	1.00	1.49	2.17
Exact[d]	2.08	1.00	0.87	1.04	0.96	0.60-1.30
$(^{3}He,d)$[e]	0.89	1.00	0.84	1.02	0.96	0.63-0.80

*Spectroscopic factors are normalized to unity for the $f_{7/2}$ state

[a]D. G. Kovar et al, Phys. Rev. Lett. 30 (1973) 1075

[b]Ref. 30

[c]Refs. 24,33

[d]Ref. 19

[e]B. H. Wildenthal et al., Phys. Rev. Lett. 19 (1967) 960.

contribute of order 20%. So within the present state of the art the simple semiclassical theory does fairly well. We now discuss its use for performing surveys, impossible to contemplate with the DWBA formulations.

We return to the energy variation, observed by the Berkeley group, shown in fig. 8. Detailed finite range DWBA calculations are not yet available. However the calculations apparently do not produce the correct energy dependence of the cross sections.[19,32] There is however a difficulty of making wide surveys, and varying optical parameters, owing to the prohibitive cost. The semiclassical calculations in post and prior forms are shown[33] in fig. 9 which gives a good overall representation of the data, including the equality of the f 7/2, f 5/2 cross sections at 200 MeV.

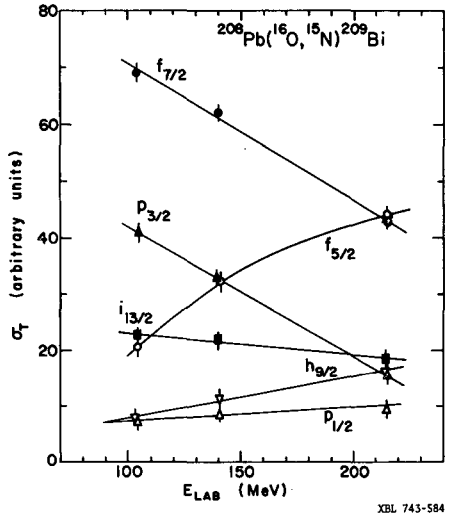

Fig. 8. Observed energy dependence of the cross sections of single particle states populated in the $^{208}Pb(^{16}O,^{15}N)^{209}Bi$ reaction (the summed cross section of all measured angles is plotted).

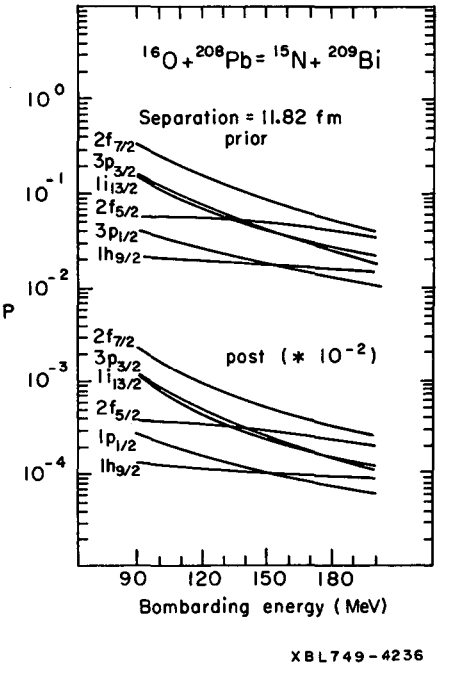

Fig. 9. Theoretical energy dependence of the semiclassical transition probability for the $^{208}Pb(^{16}O,^{15}N)^{209}Bi$ reaction, evaluated in the prior and post representations.

Both formulations have been used to study the Q-dependence of heavy-ion transfers. Buttle and Goldfarb have shown that close to the Coulomb Barrier, the optimum Q corresponds to equal distances of approach before and after transfer, as expressed by the relation[34]

$$Q_{opt} = \frac{Z_3Z_4 - Z_1Z_2}{Z_1Z_2} E_{cm} \qquad (33)$$

This relation predicts Q_{opt} = -11 MeV for the $Pb^{208}(^{16}O,^{15}N)$ reaction at 104 MeV. At this energy the proper matching conditions should balance Q to the angular momentum, mass and energy transfer. The calculations using no-recoil DWBA[11] and semi-classical[33] theory are shown in fig. 10, where we see both theories predict Q opt ≈ -6 MeV. The semiclassical calculation shows that higher ℓ-transfers peak at more negative Q-values, an effect which is not apparent in the DWBA calculations.

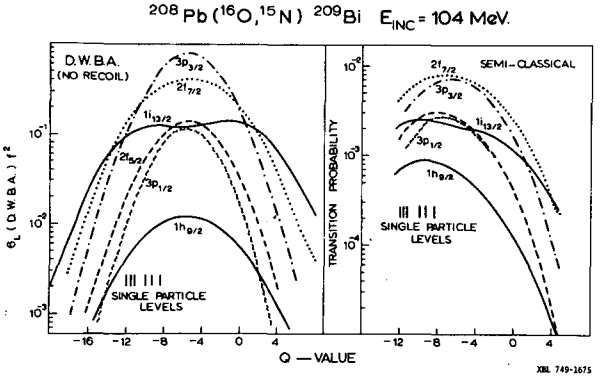

Fig. 10. Theoretical calculation of the Q-dependence for the $^{208}Pb(^{16}O,^{15}N)^{209}Bi$ reaction (a) using DWBA theory and (b) semiclassical theory. In (a) the form factor (F(r) in eq. 19) was calculated with the binding energy of the state fixed at the value for the actual single particle level, whereas in (b) the binding energy was allowed to change with Q-value.

The Q matching conditions are more transparent if we make an approximate evaluation of the space and time integrals in eq. 28,29. Then we find the probability for a transition[35] from a state $(\ell_1\lambda_1)$ to $(\ell_2\lambda_2)$ is

$$P(\lambda_2\lambda_1) \propto P_o(R) \left| Y_{\ell_1}^{\lambda_1}(\tfrac{\pi}{2},0)\, Y_{\ell_2}^{\lambda_2}(\tfrac{\pi}{2},0) \right|^2 \exp\left[-\left(\frac{R\,\Delta k}{\sigma_1}\right)^2 - \left(\frac{\Delta L}{\sigma_2}\right)^2 \right] \tag{34}$$

where

$$\Delta k = k_0 - \lambda_1/R_1 - \lambda_2/R_2 \tag{35}$$

$$\Delta L = \lambda_2 - \lambda_1 + \frac{1}{2} k_0 (R_1 - R_2) + Q_{eff}\, R/\hbar v \tag{36}$$

$$Q_{eff} = Q - (Z_1^f Z_2^f - Z_1^i Z_2^i) e^2/R. \tag{37}$$

In our previous notation $k_0 = \frac{xV}{\hbar}$, the recoil term; $P_o(R)$ depends on the radial wave functions and the distance of closest approach. The widths σ_1 and σ_2 are not precisely known but uncertainty principle estimates suggest $\sigma_1 \approx \pi$ and $\sigma_2 \approx \sqrt{\gamma R}$ where $\gamma^2 = 2x\,\varepsilon/\hbar^2$ and ε is some average of the binding energy of the transferred particle in the initial and final states. For a large transition probability

Δk, $\Delta L \approx 0$, which are the generalized kinematic conditions replacing $Q_{eff} \approx 0$ for sub-coulomb transfer. The conditions correspond to conservation of linear and angular momentum in the reaction. The total transition probability can be calculated by summing over the final magnetic substates λ_2, and averaging over the initial λ_1, weighted by angular momentum coefficents coupling the nuclear spin and angular momenta.

An application of this simple theory for ^{11}B induced reactions on ^{208}Pb at 114 MeV can be found in ref. 36. Here the increased recoil allows equal population of $j_f = \ell_f \pm 1/2$ states at lower energy. This is confirmed by the full semiclassical calculation[33] and agrees fairly well with an exact quantum mechanical calculation[14]. In the subsequent discussion of lighter nuclei we shall make use of the simple version of the semiclassical theory in eq. 34-37

4. Theory of High Energy Reactions on Lighter Nuclei

When we bombard lighter nuclei with heavy-ions, the effects of recoil increase, and are particularly dramatic for multinucleon transfer. An estimate of the importance is obtained from the condition that the angular momentum carried by the recoil momentum at the target surface be greater than one unit, or for single nucleon transfer,

$$E_L > 20 \frac{A_P}{A_T^{2/3}} \tag{38}$$

where A_P, A_T are the projectile and target mass numbers[37]. For single nucleon transfer induced by ^{12}C or ^{12}C this limit is set at 45 MeV, and for multinucleon transfer at much lower energy. In three nucleon transfer at 10 MeV/nucleon the associated transfer is $\approx 6\ \hbar$. The effect is twofold: it leads to the population high spin states; and it leads to damping of diffraction patterns in the angular distributions. This is an important point as it forces us to look for other signatures of states rather than the customary differential cross sections

To see this, it is useful to discuss a classical wave optics analogy[37]. The projectile wave scatters from a circular slit of radius R (due to localization). As it scatters it transfers angular momentum, by virtue of the momentum transfer $q = \underline{k}_i - \underline{k}_f$. (see fig. 11). In a classical model this can only change the angular momentum vector in the Z-direction, setting up L complete de Broglie wavelengths around the ring locus. The interference of waves from two characteristic spectral points A,B, will depend not only on the path difference 2d, but also on the intrinsic phase difference. For constructive interference we require:

$$2d = n\lambda \tag{39}$$

if A, B have the same relative phase, i.e. L = 0,2....., but for odd L transfer of 1,3,5 ...

$$2d = (n + \tfrac{1}{2})\lambda \tag{40}$$

So <u>odd</u> L transfers will be out of phase with even transfers.

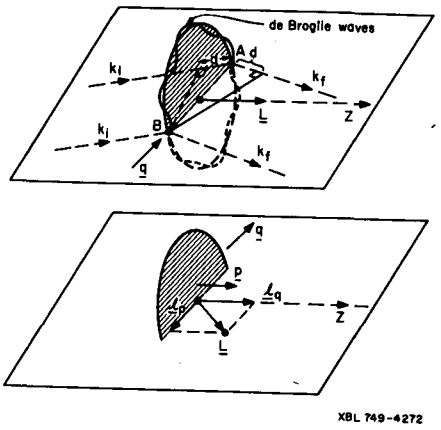

XBL 749-4272

Fig. 11. A semiclassical picture of de Broglie waves on the ring locus is illustrated at the top. Waves that emanate from A have a path difference of 2d over those from B. The bottom figure illustrates the angular momentum $\underline{\ell}q$ arising from momentum transfer q along the ring locus, and $\underline{\ell}p$ arising from the recoil effect. The total angular momentum transfer is $L = \underline{\ell}q + \underline{\ell}p$.

We have seen that recoil imparts additional momentum p, in the Z-direction, and an angular momentum ℓp perpendicular to Z, so that then the final L is made up of ℓq and ℓp, both of which take on a variety of odd and even values as θ changes. But only ℓq determines the phase of the diffractive oscillations that emanate from the ring locus. Thus the effect of ℓp is to allow even and odd ℓq and consequently in phase and out-of-phase oscillations contribute, damping the oscillatory cross-section. (compare the selection rules of eq. 26).

A striking case[38] is the $^{12}C(^{14}N,^{13}N)^{13}C$ reaction shown in fig. 12 in which the selection rules of eq. 26 allow $\Delta\ell = 0$ and $\Delta\ell = 1$ for the ground state transition, whereas the transition to the S 1/2 state allows only $\Delta\ell = 1$. As predicted above, the ground state diffraction pattern is damped, but the excited state is oscillatory albeit out of phase with the finite-range recoil calculation. It is an open question at present whether some other processes are competing here since in general the finite-range code "Lola" has been highly successful in its application to light nuclei[39]. It is clear however that recoil effects in high energy heavy-ion transfer reactions make the differential cross sections unpromising signatures in general of the properties of nuclear states. To confirm this we show in fig. 13, the collected differential cross-sections for one, two[40] and three nucleon transfers[41] induced by heavy-ions of approximately 10 MeV/nucleon. The dependence on q, the linear momentum transfer was explained by a simple recoil theory[42], using harmonic oscillator bound state wave functions, a Gaussian interaction and distorted waves replaced by amplitude

modulated plane waves, that are then evaluated using the ring locus technique.

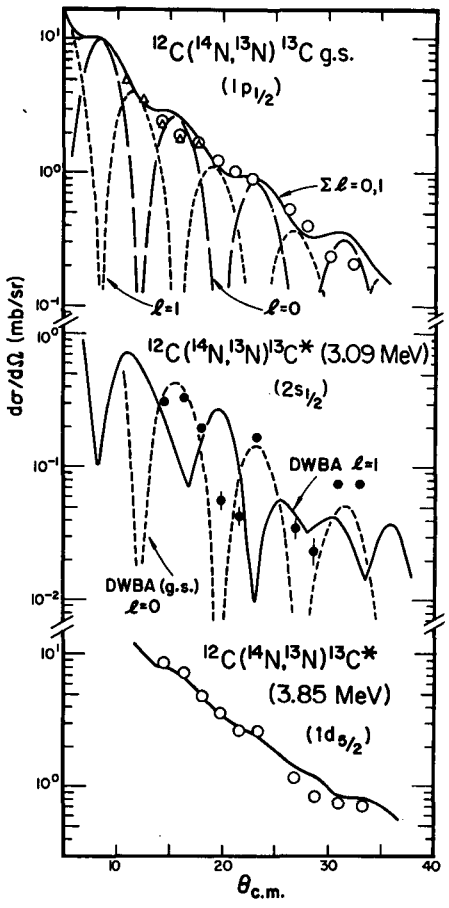

Fig. 12. Differential cross sections for the reaction $^{12}C(^{14}N,^{13}N)^{13}C$. The ground state distribution illustrates the damping of diffraction oscillations by the superposition of $\Delta\ell = 0$ and 1 transfers in the recoil DWBA calculation. The $S_{1/2}$ transition is highly oscillatory, since only one $\Delta\ell = 1$ is allowed. As discussed in the text, the phase appears better reproduced by $\Delta\ell = 0$. The DWBA agrees well with the $d_{5/2}$ transition at the bottom.

Then $$\frac{d\sigma}{d\Omega} \alpha\ q^{-3}\ \text{EXP}\left(-p^2a^2/6\right), \tag{41}$$

if $L > 1$ and $q \gg 1/a$, where a is the range of the bound state wavefunction, and p is the recoil momentum

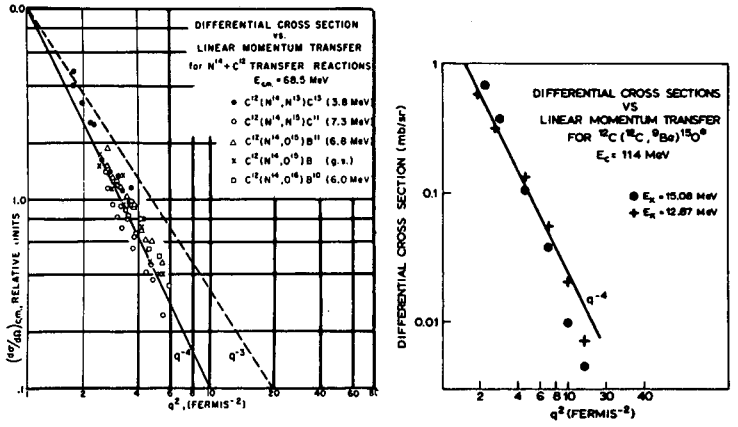

XBL 749-1674

Fig. 13. Collected differential cross sections for one, two and three nucleon transfer reactions on light nuclei induced by heavy-ion beams of approximately 10 MeV/nucleon. The data are plotted against the square of the linear momentum transfer q to remove kinematic differences. The theoretical lines q^{-3} and q^{-4} are based on an approximate recoil DWBA calculation.

The simplicity of the distributions has its compensations however. The forward rising of the cross-section suggests that the transfers occur during a grazing collision of the cores. Because of the high incident energy we may also suppose that the motion of the incident projectile is not much perturbed by the collision, so that the orbit is a straight line, with an impact parameter equal to the sum of the radii. We can then use the simple theory outlined in eq. 34-37, and compare differential cross sections at forward angles, as shown by the following considerations.

If P is the transfer transition probability, then as in the theory of Coulomb excitation we write, for cases where $\eta >> 1$,

$$(d\sigma/d\Omega) = (d\sigma/d\Omega)_{e\ell} \times P \qquad (42)$$

Also we have,

$$\sigma = 2\pi \int \left(\frac{d\sigma}{d\Omega}\right) \sin\Theta d\Theta = \frac{2\pi}{k^2} \int P(L)\,dL$$

where L is the angular momentum of relative motion. The last equation is valid if the grazing angular momentum, $kR >> 1$ and if ΔL, the contributing angular momentum range is $>> 1$. This equation does not require $\eta >> 1$. The main contribution to the first integral comes from Θ near the maximum of $\sin\Theta \frac{d\Theta}{d\Omega}$. If data on the monotonic distributions are taken near this maximum, then

$$\sigma \propto \frac{d\sigma}{d\Omega} \qquad (43)$$

since the angular distributions are similar for different final states. Similarly the main contribution to the second integral comes from L near the critical value, L_c where $P(L_c)$ has a maximum. Thus we expect, as in eq. 42, that

$$\frac{d\sigma}{d\Omega} \propto P(L_c) \tag{44}$$

will hold approximately at forward angles, even though η is not large compared to unity.

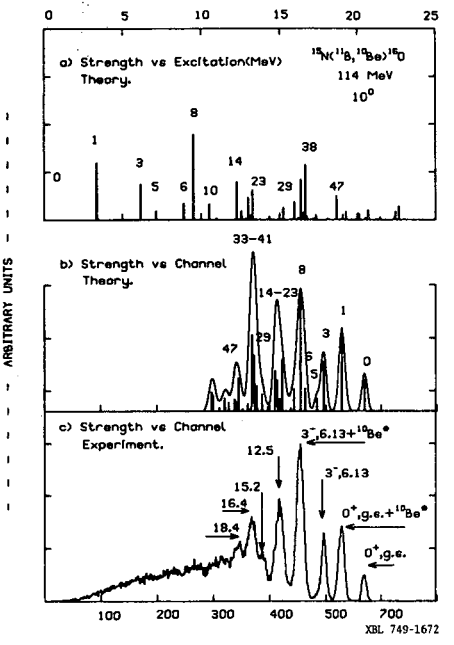

Fig. 14. (c) shows the experimental spectrum for the $^{15}N(^{11}B,^{10}Be)^{16}O$ reaction at 114 MeV; which selectively excites particle-hole-strength. (a) shows the calculated stength using shell-model spectroscopic amplitudes and the simplified semiclassical theory of eq. 34. In (b) the theoretical predictions are folded with the experimental resolution to produce a theoretical spectrum.

An application of eq. 44 combined with shell-model spectroscopic amplitudes for a survey[43] of the reaction $^{15}N(^{11}B,^{10}Be)^{16}O$ at 114 MeV is shown in fig. 14. This reaction is expected to excite preferentially the particle-hole strength in ^{16}O, formed by coupling a p 1/2, d 5/2, s 1/2 or d 3/2 particle to the ^{15}N core. Examples are the g.s., the 6.13, 3^- state, the 8.87, 2^-, the T = 1 quartet 1^-, 0^-, 2^-, 3^- analogues of ^{16}N, centered at 12.5 MeV, the 2^-_3 at 15.2 MeV etc. In addition ^{10}Be can be formed in its low lying particle stable states, but particularly the 3.37 MeV 2^+ state. The theoretical spectrum was calculated as it would appear in an experimental spectrum, each peak having a Gaussian shape of area proportional to the theoretical strength and a width equal to the average experimental value. Over 50 states were included in the calculation which automatically generated the theoretical spectra. A satisfactory representation of the data is obtained. If this method can be used for spectroscopy even within a precision of a factor of 2 or 3, it furnishes us with a powerful technique for making wide surveys in a way impossible to imagine with more elaborate theories.

More exciting of course, is the extension of this programme to two, three and four nucleon transfers. The Oxford group have shown[41,44] how these high energy heavy-ion reactions can selectively populate simple "single particle" states of ^3He or ^4He, due to the apparent preference for transfer of spatially localized clusters.[45] An example is shown in fig. 15 where it is suggested that the strongly excited states

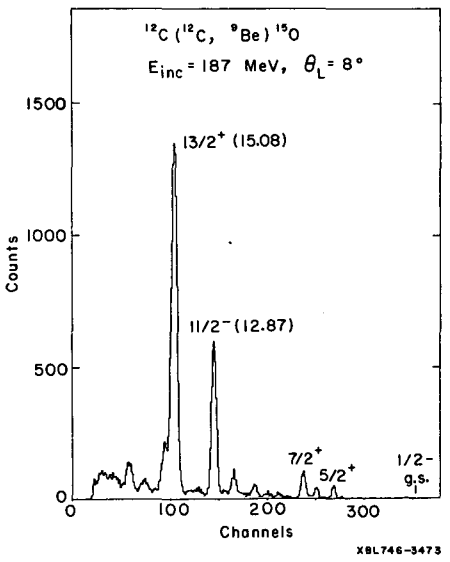

Fig. 15. Energy spectra for the ^{12}C $(^{12}C,^{9}Be)^{15}O$ reaction at 187 MeV showing the selective excitation of postulated high spin states $13/2^+$ and $11/2^-$.

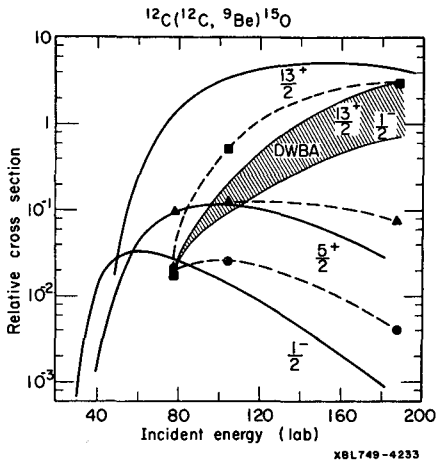

Fig. 16. The energy variation of the cross section for states excited in the $^{12}C(^{12}C,^{9}Be)^{15}O$ reaction. The solid curves are the predictions of semiclassical theory (no spectroscopic factors included) For comparison the no-recoil DWBA predictions are shown for the $1/2^-$ and $13/2^+$ states, in which there is no strong enhancement of the high spin states.

have $J^\pi = 13/2^+$ and $11/2^-$. A recent calculation using a folded potential model[46] for ^{3}He outside the ^{12}C core gives good agreement with the experimental locations for L = 6 and L = 5, ^{3}He orbitals. Table 4 gives a comparison between experiment and theory, using the methods described above, with SU_3 cluster spectroscopic amplitudes.[41] (see also the previous lecture by B. Buck).

Table IV. Comparison of experimental cross sections for the $^{12}C(^{12}C,^{9}Be)^{15}O$ reaction at 114 MeV with theoretical cross sections evaluated using a semiclassical theory for the reaction and three nucleon cluster spectroscopic amplitudes.

STATE	σ THEORY	σEXPT.
G.S. $1/2^-$	0.01	≈ 0
5.24, $5/2^+$	0.10	0.12
6.79, $3/2^+$	0.003	≈ 0
7.28, $7/2^+$	0.33	0.28
$(9.08)^a$, $9/2^+$	0.76	? STATES
$(10.80)^a$, $7/2^+$	0.29	? NOT IDENTIFIED
12.87^c, $11/2^-$	1.00^b	1.00
15.08, $13/2^+$	2.16	1.16

(continued)

TABLE IV (continued)

[a] Theoretical excitation energy

[b] Data normalized to unity for 12.87 MeV state

[c] These states were identified as $11/2^-$ and $13/2^+$ by comparison with the theory.

As new states of this type are located in other regions of the periodic table, it will be important to have methods of inferring their properties. The similarity of the distributions to different states can be turned to further advantage by studying the energy variation of the reaction at one, or a few, forward angles. The experimental variation for some states in the $^{12}C(^{12}C,^{9}Be)^{15}O$ reactions are shown in fig. 16, from recent work at Berkeley, together with the predictions of the semiclassical theory, which gives some agreement with the high energy trend, and confirms the high spin assignment of the $13/2^+$ state. For comparison we show the no-recoil DWBA predictions, using optical model parameters from a fit to the elastic scattering data at 104 MeV. The prediction was arbitrarily normalized to the $13/2^+$ state, in order to emphasize the small enhancement over the low spin $1/2^+$ state. Better agreement with the detailed shapes could be obtained using variations of the optical potentials, but the enhancement of 10^3 for $13/2^+$ compared to $1/2^-$ could only be reproduced in the DWBA calculations by including recoil. The enhancement of high spin states due to the recoil effect was demonstrated by Dodd and Greider long ago[47]. The advantages of the semiclassical theory is its ability to make wide surveys rapidly, without any unknown parameters to vary.

Many of the interesting states discovered, and awaiting discovery, in heavy-ion reactions are such high-spin states, often of small binding energy or even unbound. In the limit of small final binding energy, defined by

$$\chi_2 R_1 \ll 1 \tag{45}$$

where $\chi_2 = \sqrt{\frac{2m\varepsilon_2}{\hbar^2}}$, ε_2 is the binding energy of m in the final state and R_1 is the radius of the projectile, Nagarajan has shown[48] that the reaction proceeds almost entirely through the recoil momentum transfer, and that the six-dimensional integration of the DWBA in eq. 17 separates into:

$$T \alpha \int \underline{dr}_1 \, e^{-i\underline{k}_R \cdot \underline{r}_1} V(r_1) U_{\ell_1}(r_1) \int \underline{dr} \, e^{iq \cdot \underline{r}} \, h^*_{\ell_2}(i\chi_2 r) \, Y^{\lambda_2}_{\ell_2}(r) \times \Theta(r) \tag{46}$$

Here $U_{\ell_1}(r_1)$ is the initial radial wave function, and the final weakly bound wave function is approximated by a Hankel function. Further

$$\underline{q} = \underline{k}_i - \underline{k}_f \tag{47}$$

$$\underline{k}_R = \frac{x}{B}\underline{k}_f + \frac{x}{a}\underline{k}_i \tag{48}$$

and $\Theta(r)$ is an amplitude modulation on the plane waves to simulate distorted waves. Since eq. 48 essentially defines the recoil momentum of eq. 22, eq. 46 shows that the final result is a product of a zero-range DWBA integral with a radial integral correcting for recoil effects. The correspondence of eq. 46 with the form of the simple semiclassical theory of eq. 34 is also transparent. The spectroscopy of these new correlations in nuclear motion is likely to become a promising area of investigation with the new high energy, high resolution accelerators. The approximate forms of the exact theories outlined here will enable us to make surveys to see where the interesting regions of investigation lie.

5. Multistep Processes

In this final section, I wish to discuss some aspects of multistep processes in heavy-ion reactions at high energy. In contrast to the direct transfer reactions, so far the analyses have been done only with the coupled channels Born approximation (CCBA). However the results are sufficiently interesting and suggestive of what might be done in the future with heavier projectiles, to make us hope that soon a coupled channels semiclassical theory will be available to enable us to make the same wide surveys that have been possible for one-step direct reactions at high energies.

It has taken a long time to establish the presence of multistep processes in heavy-ion reactions, although they have been well studied in light-ion reactions. Such a case is two neutron pick-up on ^{144}Nd leading to two types of 2^+ states in ^{142}Nd. A spectrum - actually for the heavy-ion case we are about to discuss - is shown in fig. 17. The 2_2^+ state is a two neutron hole state in the N = 82 closed shell, i.e. a removal type quadrupole vibrational state, excited strongly in two neutron pick-up. The 2_1^+ state on the other hand, is dominantly a particle-hole quadrupole vibration which is forbidden in the direct pick-up. This state can be populated via the indirect routes, involving inelastic scattering shown in fig. 18. The CCBA and DWBA calculations[49] are compared for the (p,t) data in fig. 19, in which the CCBA calculation gives better agreement in magnitude for the 2_1^+ state (the forward angle phase is also better reproduced). Apart from a change in the magnitude, the effect of multistep processes is not very dramatic in this case. The same reaction induced by heavy-ions[50] is illustrated in fig. 20. Here the 0_1^+,0_2^+, and 2_2^+ all have the well-known, bell-shaped distribution, which is the characteristic of direct reactions with heavy-ions. The 2_1^+ state has no such "semi-classical" maximum, but is flat and rises at forward angles. Tamura and Low have suggested[51] how this forward rise, due to indirect

processes, can be understood on a semiclassical trajectory picture. In fig. 21, we see that a nucleus deviated from its spherial shape (by for example inelastic scattering) for a given impact parameter makes a closer collision and thereby is deflected to more forward angles by the nuclear force. These results have been reproduced by CCBA calculations[50]. This example is a good "control" case for demonstrating indirect effects, because the direct 2_2^+ distribution must be reproduced simultaneously.

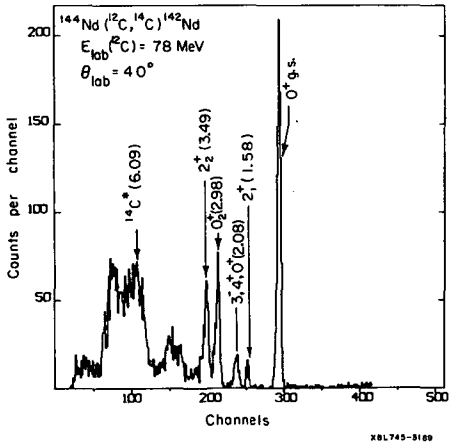

Fig. 17. Spectrum for the ^{144}Nd(^{12}C,^{14}C)^{142}Nd reaction at 78 MeV, showing the population of two different types of 2^+ states; the 2_1^+ state is a particle-hole vibration, forbidden in direct pick-up and the 2_2^+ which is more strongly excited is a two-neutron hole state.

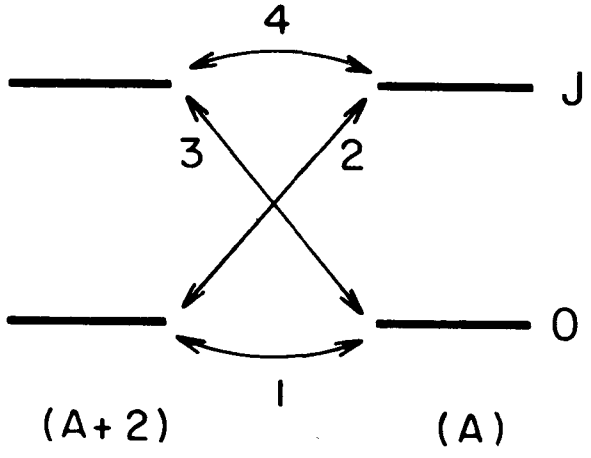

XBL 739-1244

Fig. 18. Illustration of direct and indirect routes in transfer reactions. In two neutron pick-up to the state J route 2 is direct and in stripping 3 is direct. The opposite sign of 2 and 3 can lead to opposite interference characteristics with indirect routes of which 4 and 1 are branches.

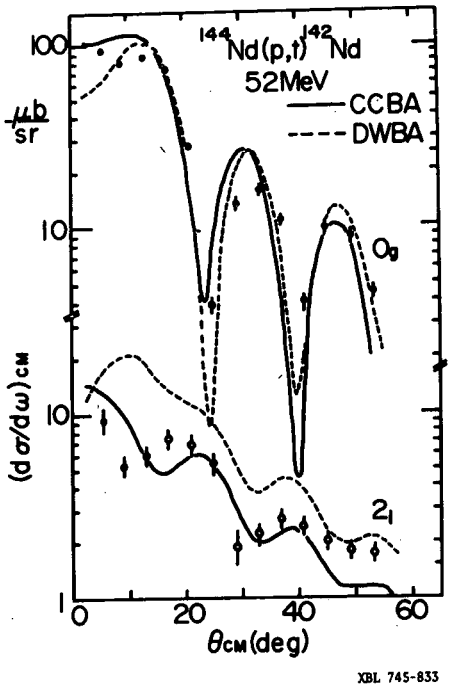

Fig. 19. Comparison of DWBA and CCBA calculations for the $^{144}Nd(p,t)^{142}Nd$ reaction. The CCBA gives better agreement in magnitude and phase for the weakly excited 2^+ state.

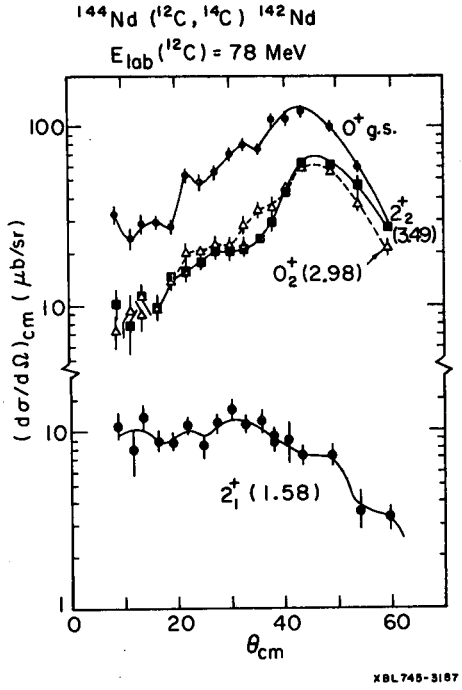

Fig. 20. Differential cross sections for the $^{144}Nd(^{12}C,^{14}C)\ ^{142}Nd$ reaction at 78 MeV. The $0^+_{g.s}$, 0^+_2 and 2^+_2 distributions all exhibit the semiclassical maximum characteristic of a direct reaction, whereas the weakly excited 2^+_1 has no clear peak and rises at forward angles.

Using this signature of the indirect transition, we can study an interesting effect which has not, to my knowledge, been studied in light-ion reactions. The interference between direct and indirect modes to the lowest 2^+ vibrational states in the Sn isotopes is predicted to be constructive in the pick-up (^{16}O,^{18}O) reaction and

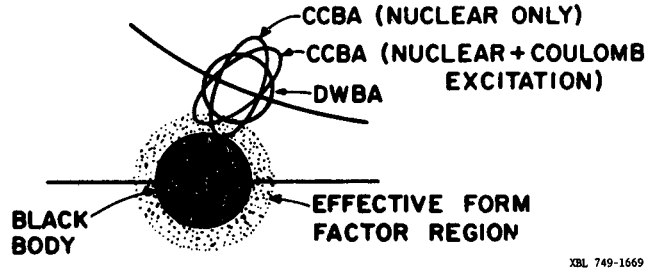

Fig. 21. Semiclassical interpretation of forward rising differential cross sections in indirect transitions, due to the closer interaction of nuclei deformed from their spherial shape.

destructive in the (^{18}O,^{16}O) stripping reaction[52]. Data for these reactions[53] at the same center of mass energy are shown in fig. 22. The cross sections for the ground states are identical as required by time-reversal invariance and exhibit the classical maximum, as does the cross-section for the 2^+ state in pick-up. The 2^+ in stripping however is flattened in the same way as the data on niodymium. The theoretical calculations are shown in fig. 23. Here the interference is sufficiently strong to produce a dip which does not appear in the data, but the magnitude of this effect is sensitive to deformations, nuclear structure and optical parameters. The figure also shows the result of neglecting higher order effects in the calculation, when <u>all</u> the distributions assume the same form. In a recent study of the $^{186}W(^{12}C,^{14}C)^{184}W$ reaction at 70 MeV, the interference effects <u>do</u> produce a dip in the differential cross-section[54]. Finally it is interesting to note that for the Sn case, the effect is one of higher energies, since at 72 MeV, it disappears[55]. Heavy-ion reactions are rich in possibilities for the study of interference effects, and clearly we are seeing only the beginning of an area of research which may yield spectacular results in the future, as heavier projectiles are involved.

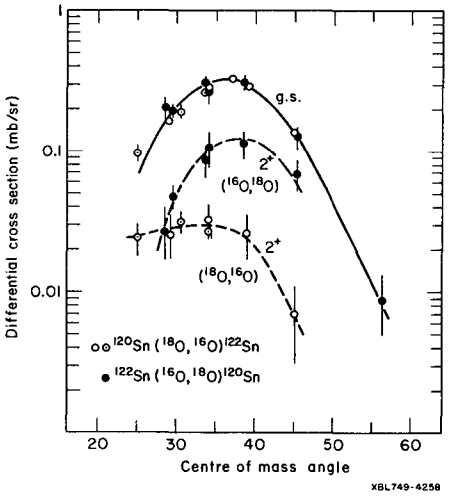

Fig. 22. Differential cross sections for the reaction $^{120}Sn(^{18}O,^{16}O)^{122}Sn$ and $^{122}Sn(^{16}O,^{18}O)^{120}Sn$ at the same center of mass energies of 89 MeV. Destructive interference between direct and indirect routes to the 2^+ state in stripping leads to an anomalous distribution.

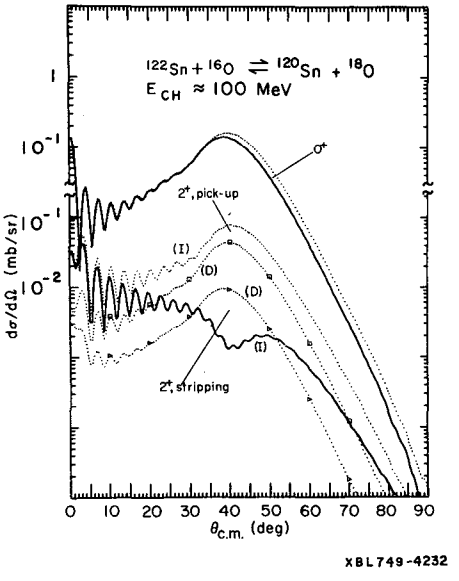

Fig. 23. Theoretical predictions for the $^{120}Sn(^{18}O,^{16}O)^{122}Sn$ and $^{122}Sn(^{16}O,^{18}O)^{120}Sn$ reactions. For the 2^+ states both CCBA calculation (I) and DWBA calculation (D) are compared.

6. Conclusion

In this talk, I have presented some of the approaches to the analysis of high energy transfer reactions with heavy-ions, concentrating on concrete achievements at the present time rather than on the possiblities in sight on the horizon. First we discussed the use of simple semiclassical concepts in the physical interpretation of various features of differential cross sections. Reliance on full quantal theories in this area often lead to what Glendenning has called[2] the "experimental approach" in which a parameter, of the optical potential for example, is varied and its effect catalogued and noted. A more formal semiclassical theory was compared with the exact and approximate DWBA theories for reactions where the semiclassical assumptions were well fullfilled. The power of the method in making rapid surveys of effects such as energy and Q-dependence was demonstrated. In this way one can determine what are the interesting areas to investigate experimentally. This was followed by a discussion of transfers on lighter nuclei where heavy-ion reactions have been used to give us information on new states and correlations in nuclear motion. The final discussion of the indirect effects in multistep processes at high energy gives us a glimpse of new areas of research unique to heavy ions in which semiclassical theories are likely to play an increasingly important role.

This discussion has left untouched the many technical developments in progress which are transforming the semiclassical approach from a crude approximation to a refined theory. These methods calculate a semiclassical scattering amplitude which gives a proper account of interference and diffractive phenomena in heavy-ion physics[31]. These approaches can go beyond the geometric optics limit towards wave optics allowing for complex trajectories which describe quantal phenomena in terms of classical quanities[56,57]. In this spirit the semiclassical approach becomes more and more useful at higher incident energies. In the high energy limit the Glauber or eikonal approaches[58] will become possible, and there have already been some successes in this direction[59,60,61].

Since we are now entering an era of higher energies and higher mass projectiles, we are likely to encounter situations with an enormous number of partial waves, hundreds or even thousands. Here the semiclassical approach may become our only hope of making theoretical progress. Or more aesthetically we shall probably have to combine semi-classical and quantal theories, using quantum mechanics to calculate the S matrix up to the region of critical angular momentum where the nuclear field causes rapid changes in the deflection function, with classical methods in the wider region where S waves smoothly[2].

I wish to thank the experimental and theoretical heavy-ion groups at Berkeley and Oxford for supplying me with many ideas and data.

References

*Work performed under the auspices of the U. S. Atomic Energy Commission.

1) K. W. Ford and J. A. Wheeler, Ann. Phys. (N.Y.) 7 (1959) 259
2) N. K. Glendenning, Proceedings of the Conference on the Interactions of Complex Nuclei (Nashville, 1974) Vol 2, to be published.
3) V. M. Strutinskii, Sov. Phys. JETP 19 (1964) 1401
4) L. D. Landau and E. M. Lifshitz, Quantum Mechanics. (Pergamon Press Ltd, London, 1958)
5) J. Grabowski, B. N. Kalinkin and N. F. Markova, Nuc. Phys. 65 (1965) 294
6) F. A. Gareev, J. Grabowski and B. N. Kalinkin Sov. J. of Nuc. Phys. 5 (1967) 85
7) S. Kahana, P. D. Bond and C. Chasman, Phys. Lett. 50B (1974) 199
8) V. M. Strutinskii, Phys. Lett. 44B (1973) 245
9) P. J. Siemens and F. D. Becchetti, Phys. Lett. 42B (1972) 389
10) J. S. Larsen, J. L. C. Ford, R. M. Gaedke, K. S. Toth, J. B. Ball and R. L. Hahn, Phys. Lett. 42B (1972) 205
11) D. G. Kovar, Symposium on Heavy-Ion Transfer Reactions (Argonne, 1973) p. 59
12) W. von Oertzen, Symposium on Heavy-Ion Transfer Reactions (Argonne, 1973) p. 675
13) K. S. Low and T. Tamura, Phys. Lett. 48B (1974) 285
14) J. L. C. Ford, K. S. Toth, G. R. Satchler, R. M. Devries, R. M. Gaedke, P. J. Riley and S. T. Thornton, Phys Rev. (C), to be published.
15) F. D. Becchetti, D. G. Kovar, B. G. Harvey, J. Mahoney, B. Mayer and F. G. Pühlhofer Phys. Rev. C6 (1972) 2215
16) G. C. Morrison, J. de. Physique 32, 11-12 (1971)
17) R. J. Asciutto and N. K. Glendenning, Phys. Lett. 48B (1974) 6
18) W. A. Friedman, K. W. McVoy and G. W. T. Shuy, Phys. Rev. Lett. 33 (1974) 308
19) D. G. Kovar, F. D. Becchetti, B. G. Harvey, D. L. Hendrie, H. Homeyer, J. Mahoney and W. von Oertzen, Nuclear Chemistry Annual Report (1973) LBL-2366, p 94
20) J. S. Blair, R. M. Devries, K. G. Nair, A. J. Baltz and W. Reisdorf, to be published.
21) N. K. Glendenning and M. A. Nagarajan, LBL-2378 Preprint (1974) and to be published.
22) G. R. Satchler, Symposium on Heavy-Ion Transfer Reactions (Argonne, 1973) p 145 and references therein.
23) R. A. Broglia and A. Winther, Physics Reports 4C (1972) 153 and refs. therein.
24) D. M. Brink, P. N. Hudson and M. Pixton, to be published.
25) M. A. Nagarajan, Nuc. Phys. A196 (1972) 32; A209 (1973) 485
26) A. J. Baltz and S. Kahana, Phys. Rev. C9 (1974) 2243
27) E. Elbaz, J. Meyer and R. S. Nahabetian, Nuc. Phys. A205 (1973) 299
28) B. F. Bayman and D. H. Feng, Nuc. Phys. A205 (1973) 513
29) L. A. Charlton, Phys. Rev. Lett. 31 (1973) 116; Symposium on Heavy-Ion Transfer Reactions (Argonne, 1973) p 161
30) T. Tamura and K. S. Low, Phys. Rev. Lett. 31 (1973) 1356
31) R. A. Broglia, S. Landowne, R. A. Malfliet, V. Rostokin and A. Winther, Phys. Reports C11 (1974) 1
32) D. G. Kovar, private communication, 1974
33) P. N. Hudson, D. Phil Thesis (Oxford, 1973)
34) P. J. A. Buttle and L. J. B. Goldfarb, Nuc. Phys. A115 (1968) 461
35) D. M. Brink, Phys. Lett. 40B (1972) 37
36) N. Anyas-Weiss, J. Becker, T. A. Belote, J. C. Cornell, P. S. Fisher, P. N. Hudson, A. Menchaca-Rocha, A. D. Panagiotou and D. K. Scott, Phys. Lett. 45B (1973) 231
37) K. R. Greider in Nuclear Reactions Induced by Heavy-Ions, ed. by R. Bock and W. R. Hering (North Holland, Amsterdam, 1970) p 217
38) R. M. Devries, M. S. Zisman, J. G. Cramer, K-L Liu, F. D. Becchetti, B. G. Harvey, H. Homeyer, D. G. Kovar and W. von Oertzen, Phys Rev. Lett. 32 (1974) 680

39) R. M. Devries, Phys. Rev. C8 (1973) 951
40) J. Birnbaum, J. C. Overley and D. A. Bromley, Phys. Rev. 157 (1967) 787
41) N. Anyas-Weiss, J. C. Cornell, P. S. Fisher, P. N. Hudson, A. Menchaca-Rocha, D. J. Millener, A. D. Panagiotou, D. K. Scott, D. Strottman, D. M. Brink, B. Buck, P. J. Ellis and T. Engeland, Physics Reports C, to be published.
42) L. R. Dodd and K. R. Greider, Phys. Rev. 180 (1968) 1187
43) A. Menchaca-Rocha, D. Phil. Thesis (Oxford, 1974) and A. Menchaca-Rocha et al.,to be published.
44) D. K. Scott, P. N. Hudson, P. S. Fisher, N. Anyas-Weiss, C. U. Cardinal, A. D. Panagiotou, P. J. Ellis and B. Buck, Phys. Rev. Lett. 28 (1972) 1659
45) D. Kurath, Lectures at International School of Physics, Enrico Fermi, Varenna 1974, to be published
46) B. Buck, C. B. Dover and J. P. Vary, to be published.
47) L. R. Dodd and K. R. Greider, Phys. Rev. Lett. 14 (1965) 959
48) M. A. Nagarajan, LBL-2918 (Preprint 1974) and to be published.
49) K. Yagi, K. Sato and Y. Aoki, T. Udagawa and T. Tamura, Phys. Rev. Lett. 29 (1972)
50) K. Yagi, D. L. Hendrie, L. Kraus, C. F. Maguire, J. Mahoney, D. K. Scott, Y. Terrien, T. Udagawa, K. S. Low and T. Tamura, to be published.
51) K. S. Low and T. Tamura, Symposium on Heavy-Ion Transfer Reactions (Argonne, 1973) p 655
52) R. J. Ascuitto and N. K. Glendenning Phys. Lett. 45B (1973) 85
53) D. K. Scott, B. G. Harvey, D. L. Hendrie, U. Jahnke, L. Kraus, C. F. Maguire, J. Mahoney, Y. Terrien, K. Yagi and N. K. Glendenning, to be published.
54) K. A. Erb, private communication, 1974
55) H. G. Bohlen and H. J. Körner, private communication, 1974
56) J. Knoll and R. Schaeffer, Lectures at the International Center for Theoretical Physics (Trieste, 1973) to be published.
57) R. Malfliet, this Symposium.
58) R. J. Glauber, Lectures in Theoretical Physics, Boulder, Vol 1 (Interscience Publishers, N. Y. 1959) p 315.
59) A. Dar and Z. Kirzon, Phys. Lett. 37B (1971) 166
60) R. da Silveira J. Galin and C. Ngo, Nuc. Phys. A159 (1970) 481
61) B. Buck, private communication, 1974

TECHNICAL INFORMATION DIVISION
LAWRENCE BERKELEY LABORATORY
UNIVERSITY OF CALIFORNIA
BERKELEY, CALIFORNIA 94720